Scrapie Amyloid (Prion) Protein Has the Conformational Characteristics of an Aggregated Molten Globule Folding Intermediate

Jiri Safar,*,‡ Peter P. Roller,§ D. Carleton Gajdusek,‡ and Clarence J. Gibbs, Jr.‡

Laboratory of Central Nervous System Studies, National Institute of Neurological Disorders and Stroke, and Laboratory of Medicinal Chemistry, DTP, DCT, National Cancer Institute, National Institutes of Health, Bethesda, Maryland 20892

Received January 14, 1994; Revised Manuscript Received April 6, 1994®

ABSTRACT: The scrapie amyloid (prion) protein (PrP27–30) is a host-derived component of the infectious scrapie agent; the potential to replicate, propagate, and form amyloid is a result of the posttranslational event or conformational abnormality. In low concentrations of guanidine hydrochloride (Gdn·HCl), PrP27–30 dissociates into a compact equilibrium intermediate with a substantial portion of secondary structure, partially denatured tertiary structure, and tryptophan residues in an apolar environment [Safar, J., Roller, P. P., Gajdusek, D. C., & Gibbs, C. J., Jr. (1993) *J. Biol. Chem. 27*, 20276–20284]. Here we describe the characteristics of this metastable form as monitored by 8-anilino-1-naphthalenesulfonate (ANS) fluorescence spectroscopy and circular dichroism (CD) spectroscopy, and we propose a mechanism for scrapie amyloid association. The Gdn·HCl-induced equilibrium intermediate of PrP27–30 had multiple high-affinity hydrophobic binding sites for ANS, some close to the Trp residues. The amide CD spectrum of an acid-induced intermediate (A-form), in equilibrium at pH <2.0, was similar to the Gdn·HCl-induced intermediate and suggested the presence of a significant portion of an α-helical or β-turn secondary structure. In contrast, the PrP27–30 associated into aggregates in an all-β-sheet conformation with less ordered and more exposed hydrophobic side chains. The noncooperative unfolding of the Gdn·HCl-induced intermediate at high temperature was irreversible and correlated with the loss of infectivity. The results demonstrate that PrP27–30 associates through a compact, metastable hydrophobic intermediate with a nonnative, nondenatured secondary structure and a tertiary structure close to the unfolded form. The molten globule-like characteristics suggest that the scrapie amyloid (prion) protein is an aggregated form of an equilibrium intermediate or an early kinetic intermediate of PrP folding pathways.

Scrapie amyloid (prion) protein plays a key role in the transmission and pathogenesis of spongiform encephalopathies and is a critical factor in neuronal degeneration. The protein transformation, triggered by the disease, is a three-stage process: normal form of scrapie amyloid precursor (cellular isoform of prion protein, PrP^{C})[1] → the infectious form (scrapie isoform of prion protein, PrP^{Sc}) → the scrapie amyloid (prion protein, PrP27–30) (Gajdusek, 1988; Prusiner, 1993). Such a cascade occurs not only in scrapie in sheep and goat but also during the development of encephalopathy in mink, chronic wasting disease in deer and elk, bovine spongiform encephalopathy (BSE) in cattle, and Creutzfeldt–Jakob disease (CJD), kuru, Gerstmann–Sträussler–Sheinker syndrome (GSS), and fatal familial insomnia in humans (Gajdusek, 1988; Prusiner, 1993; Weissmann, 1991).

The chemical and molecular biological evidence demonstrates that the PrP^{Sc} protein is an isoform of the host cell-derived PrP^{C} protein (Prusiner, 1993). PrP^{Sc}, compared with PrP^{C}, has an abnormal membrane interaction (Safar et al., 1991; Stahl et al., 1990), distinctly different physicochemical behavior, the potential to form amyloid (Prusiner et al., 1983), and different secondary structure (Pan et al., 1993; Safar et al., 1993a). Both PrP^{C} and $PrP^{Sc/CJD}$ protein isoforms are encoded by the same cellular gene, and until now, chemical differences between these proteins have not been identified [for a review, see Prusiner (1993)]. Therefore, it is possible that amyloid formation and disease transmission result from conformational transitions in the PrP molecule. The thermodynamics of such a process could be facilitated by point mutations in the PrP molecule or by a hypothetical ligand.

The intrinsic insolubility and aggregated, polymer-like state of PrP27–30 and other amyloids make it very difficult to directly examine the mechanism of association, as well as their secondary and tertiary structure. Due to the lack of techniques, most of the currently available data relate to the secondary structure or synthetic peptide models, and the resulting concepts are restricted to that structural level (Glenner & Murphy, 1989; Lansbury, 1992). However, scrapie and all other amyloids have monomeric conformational precursors with stable native secondary and tertiary structure, which must have been formed through distinct steps and intermediates (Creighton, 1990; Jaenicke, 1991; Matthews, 1993b). Thus, the critical problem of amyloid formation may not be the formation of "cross-β"-sheet secondary structure *de novo*, but rather how the native secondary and tertiary structure of a precursor protein transforms or collapses into the amyloid aggregate and how this alternative folding pathway is related to that of a precursor.

The rapidly expanding experimental data corroborate the framework concept of protein folding and demonstrate that monomeric and oligomeric proteins fold through distinct intermediates with nonnative secondary and tertiary structure (Matthews, 1993b). Formation of the quaternary structure

* Corresponding author: Dr. Jiri Safar, Laboratory of Central Nervous System Studies, National Institute of Neurological Disorders and Stroke, NIH, Bldg 36, Room 4A-15, Bethesda, MD 20892.

‡ National Institute of Neurological Disorders and Stroke.

§ National Cancer Institute.

® Abstract published in *Advance ACS Abstracts,* June 15, 1994.

[1] Abbreviations: ANS, 8-anilino-1-naphthalenesulfonate; CD, circular dichroism spectroscopy; Gdn·HCl, guanidine hydrochloride; PrP^{C}, normal cellular isoform of prion protein; $PrP^{Sc/CJD}$, scrapie (Sc) or Creutzfeldt–Jakob disease (CJD) isoform of prion protein; PrP27–30, prion protein; SE–HPLC, size-exclusion high-pressure liquid chromatography; TBS, 10 mM Tris and 100 mM NaCl; [θ], mean residue ellipticity.

0006-2960/94/0433-8375$04.50/0

(aggregates), coupled with the assembly of the β-sheet-like secondary structure in scrapie and other amyloids, adds an additional layer of complexity to the problem of determining the mechanism by which a specific amino acid sequence directs folding into a unique conformation (Jaenicke, 1987; Mann & Matthews, 1993). The development of this higher-order structure raises several questions not encountered in the folding of monomeric proteins: (a) What is the secondary and tertiary structure of the scrapie amyloid monomer prior to aggregation? (b) Does the change in secondary and/or tertiary structure occur before, during, or after association, and what is the kinetic and thermodynamic relationship? (c) At what kinetic and thermodynamic intermediate step of the normal folding pathway(s) does the transition occur? (d) If the native protein can form both normal monomers of PrP^{C} and abnormal aggregates of PrP^{Sc}, where in the reaction pathway is the critical crossroad? (e) At what stage of the above transitions and how can replication and propagation occur?

The equilibrium dissociation and unfolding of PrP27–30 presented in our previous paper (Safar et al., 1993a) addressed some of the above questions, and the results are best described as $A \leftrightarrow I_1 \leftrightarrow I_2 \leftrightarrow U$, where A is an aggregate, I_1 and I_2 are equilibrium intermediates, and U is the unfolded form of the protein. The scrapie amyloid-dissociated intermediate I_1 had a substantial portion of ordered secondary structure and a tertiary structure close to that of the unfolded form (Safar et al., 1993a). In the present paper, we further characterize this monomeric, amyloid-forming equilibrium intermediate of PrP27–30 by monitoring the dissociation and unfolding of PrP27–30 by 8-anilino-1-naphthalenesulfonate (ANS) fluorescence spectroscopy and by both far- and near-UV CD spectroscopy during the perturbation of pH and temperature. The results indicate that the scrapie amyloid (prion) protein forms through a monomeric intermediate with the following conformational characteristics: (a) native-like Stokes' radius (Safar et al., 1993a); (b) substantial portion of secondary structure [this paper and Safar et al. (1993a)]; (c) little or no tertiary structure interactions and Trp in an apolar environment (Safar et al., 1993a); (d) higher affinity for ANS than in the unfolded state; and (e) noncooperative and, for different CD wavelengths, noncoincident temperature-induced unfolding of the secondary and residual tertiary structure. The characteristics of this dissociation intermediate of PrP27–30, in equilibrium in low Gdn·HCl concentrations and at low pH, are those of the early folding intermediates of the protein folding pathway (Matthews, 1993b) and it is assigned as a compact intermediate (Creighton, 1990) or a molten globule (Kuwajima, 1989).

MATERIALS AND METHODS

Source of Hamster PrP^{Sc} and PrP27–30. Golden Syrian hamsters LVG/LAK (Animal Production Area, Frederick Cancer Research Facility, Frederick, MD) were inoculated intracerebrally (ic) with 0.03 mL of a 10^{-2} dilution of hamster brain homogenate infected with the seventh serial hamster passage of scrapie strain 263K. All animals were sacrificed during the advanced terminal stage of their illness, and their brains were surgically removed under aseptic conditions, snap-frozen, and stored at −70 °C until use.

Bioassay. The infectivity assay was carried out using groups of eight weanling female golden Syrian hamsters LVG/LAK (Animal Production Area, Frederick Cancer Research Facility, Frederick, MD) inoculated ic with 0.03 mL of a 10^{-2} or 10^{-3} dilution of the test sample in phosphate-buffered saline (PBS, pH 7.4). The clinical diagnosis of scrapie was confirmed by a histopathological evaluation of two randomly chosen hamster brains from each test sample. The titers were calculated from the incubation time as described (Safar et al., 1993a).

Purification of Hamster PrP^{Sc} and PrP27–30. The purification procedure of PrP^{Sc} is described in detail elsewhere (Safar et al., 1990, 1993a). To cleave PrP^{Sc}, the protein was resuspended in PBS (pH 7.4) containing 2.3 M NaCl and 1% sarcosyl (w/v) to a final protein content of 1 mg/mL and incubated with proteinase K (27 units/mg activity; Merck, Darmstadt, Germany) for 2 h at 37 °C at an enzyme:protein ratio of 1:40 (w/w). The reaction was stopped by adding 3 mM PMSF and aprotinin and leupeptin, 20 and 10 μg/mL each, respectively; the sample was centrifuged at 13000*g* (Beckman SW 55 rotor) for 15 min at 4 °C. The pellet was washed first in H_2O containing 0.1% sarcosyl, 2 μg/mL aprotinin, and 1 μg/mL leupeptin, then in TBS (pH 7.4) containing 2 μg/mL aprotinin and 1 μg/mL leupeptin, and then in TBS (pH 7.4) only.

Protein Content. Protein content was calculated from the absorption coefficient ϵ_{205} (1 mg/mL, 1 cm) and the absorbance at 205 nm as described (Safar et al., 1993c; Scopes, 1974; Stevens, 1977) or by BCA protein assay (Pierce, Rockford, IL). The standard solutions for ϵ_{205} determination and BCA assay were prepared from SE-HPLC-purified PrP27–30 after protein determination by amino acid analysis as described (Safar et al., 1993a). The CD spectrum was recorded in parallel with an HT parameter, and absorbance was calculated by the software provided by the manufacturer (Jasco Inc., Easton, MD).

Circular Dichroism (CD) Spectroscopy. Measurements were carried out in a 1-mm path length quartz cell (Hellma Cells Inc., Jamaica, NY) with a Jasco spectropolarimeter Model J-720/IBM PS2 (Jasco Inc., Easton, MD) and are expressed as the mean residue ellipticity, $[\theta]$. The recording parameters were as follows: bandwidth, 1.0 nm; slit width, auto; sensitivity, 2–5 mdeg; response, 4 s; scan speed, 10 nm/min; and step resolution, 0.025 nm. The mean residue weight calculated according to the DNA-deduced amino acid sequence starting at Gly90 minus the carboxyl-terminal domain is 109.5 for hamster PrP27–30.

The films were prepared as previously described (Safar et al., 1993a,c), and the CD spectra are the averages of 2–4 scans with the baseline subtracted from corresponding blanks. Briefly, the PrP27–30 was sonicated 5× in 5-s bursts at 50 W on ice using a BraunSonic 2000 and a microprobe and dialyzed for 24 h at 4 °C against three changes of H_2O. The film was cast onto 0.01-cm path length quartz square sandwich cells by loading 0.9 nmol of the protein in 100 μL of H_2O. The films were dried under vacuum in a desiccator for 24 h. The protein content in the film was calculated from the absorbance at 205 nm as described. Reproducible CD spectra were obtained for samples stored at 4 °C under N_2. The 90° and 180° rotations of the film orthogonal to the beam axis did not change the spectrum of PrP27–30 (data not shown) or other model proteins (Safar et al., 1993c). The data shown are representative spectra from 2–4 experiments.

ANS and Tryptophan Fluorescence Spectroscopy. The concentration of ANS was determined by using a molar extinction coefficient of 6.8×10^3 M^{-1} cm^{-1} at 370 nm in methanol (Mann & Matthews, 1993). Fluorescence spectra were recorded with a Perkin-Elmer Model MPF-66 spectrofluorometer in 5-mm path length quartz cells (Hellma Cells Inc., Jamaica, NY). For dissociation/unfolding experiments, the samples at a protein concentration of 4.3 μM were

equilibrated for 24 h in 0–7 M Gdn·HCl in TBS (pH 7.4), as described (Safar et al., 1993a), and diluted 4× with buffer containing the corresponding Gdn·HCl concentration and finally 125 μM dye immediately before fluorescence spectroscopy. The excitation and emission wavelengths of ANS used were 380 and 490 nm, respectively.

For ANS fluorescence titration, 0.5–5-μL aliquots of concentrated stock solutions of ANS were added to the 0.5-mL cuvette containing a 4.3 μM concentration of PrP27–30 and previously equilibrated for 24 h in 2 M Gdn·HCl. The tryptophan fluorescence emission spectra were measured with an excitation wavelength of 292 nm with a 5-nm slit. Intensity and wavelength maxima were determined after subtracting the background from the corresponding blanks.

The binding data for an increasing ANS concentration and a constant protein concentration (P_0) were fit by the least-squares regression program into the following formula (Cogan et al., 1976):

$$P_0\alpha = [1/n][L_0\alpha/(1-\alpha)] - [K_D/n] \quad (1)$$

where P_0 is the total protein concentration, L_0 is the total ligand concentration, K_D is the apparent dissociation constant in the presence of 2 M Gdn·HCl, and n is the number of binding sites. α, the fraction of binding sites remaining free, is assumed to be equal to $(FI_{max} - FI)/FI_{max}$, where FI_{max} is the fluorescence intensity when all protein molecules are saturated by the ligand.

Quenching of the intrinsic tryptophan fluorescence of PrP27–30 by ANS was monitored by a Stern–Volmer plot and analyzed by fitting the data by the nonlinear least-squares program into the following formula (Eftink & Ghiron, 1976):

$$F_0/Fe^{V[Q]} = 1 + K_{SV}[Q] \quad (2)$$

where F and F_0 are the tryptophan fluorescence intensities with and without quenching, respectively, K_{sv} is the Stern–Volmer quenching constant, V is the static quenching constant (Eftink & Ghiron, 1976), and [Q] is the concentration of ANS.

Equilibrium Dissociation and Unfolding in HCl and Gdn·HCl. Aliquots of PrP27–30 from stock in TBS (pH 7.4) were diluted manually to the final concentration of Gdn·HCl or HCl with a constant 4.3 μM concentration of the protein. The pH was determined at 23 °C by a pH meter equipped with a microprobe. The Gdn·HCl-containing samples were equilibrated for 24 h at 23 °C; HCl-treated samples were recorded immediately. The stock solution of 8 M Gdn·HCl in TBS (pH 7.4) was prepared as previously described (Pace, 1986). Dissociation and unfolding were followed by monitoring the turbidity at 350 nm, by CD spectroscopy, and by ANS and tryptophan fluorescence spectroscopy (see above). Turbidity was measured with a Beckman Model DU-68 spectrophotometer in a 0.1-cm optical path length cell at 350 nm at 23 °C against blanks with identical buffer and Gdn·HCl composition and at a protein concentration of 4.3 μM.

The raw data from each assay were converted into the apparent fractional change of dissociation/unfolding (Matthews & Crisanti, 1981):

$$F_{app} = (Y_{obsd} - Y_N)/(Y_U - Y_N) \quad (3)$$

where Y_{obsd} is the observed value of the parameter and Y_N and Y_U are the values of the parameter for the native and unfolded forms, respectively, at the given Gdn·HCl concentration (Matthews & Crisanti, 1981).

Temperature-Induced Unfolding. Aliquots with a 4.3 μM concentration of PrP27–30 were equilibrated for 24 h at 23 °C in 2 M Gdn·HCl in TBS (pH 7.4) and degassed in a vacuum. CD spectra were measured in a cylindrical, 1-mm path length, water-jacketed quartz cell (Hellma Cells Inc., Jamaica, NY) connected to the circulation bath. The temperature was measured by a thermistor on the cell and controlled through the interface by IBM/PS2 and temperature control software (Jasco Inc., Easton, MD).

SDS-PAGE and Densitometry. SDS–PAGE and silver staining of the electrophoresed proteins are described elsewhere (Safar et al., 1990). The gels were scanned using a Shimadzu Model CS-9000 dual-wavelength flying-spot laser scanner in the linear transmittance mode at 550 nm.

Reagents. Ultrapure Gdn·HCl was purchased from Schwarz/Mann (Cleveland, OH) and used without further purification. ANS was obtained from Fluka (>98%, Ronkonkoma, NY). All other chemicals were reagent grade and of the highest purity commercially available.

RESULTS

Properties and Purity of PrP27–30. As estimated from the densitometry of silver-stained gels (not shown), the purity of PrP27–30 was ~95%. The triplet bands on silver-stained gels and Western blots reflect different levels of glycosylation (Turk et al., 1988). The infectivities of different states of PrP27–30 were as follows: sonicated suspension, 8.4 ± 0.1 (x ± SEM) log ID_{50}/mL; reconstituted film, 8.7 ± 0.3 log ID_{50}/mL; and sample diluted 1000× from 2 M Gdn·HCl solution, 8.1 ± 0.3 log ID_{50}/mL. The results are similar to those reported elsewhere (Safar et al., 1993a); the differences are not statistically significant.

Changes in ANS Fluorescence with Equilibrium Dissociation/Unfolding of PrP27–30 in Gdn·HCl. The fluorescence spectrum of ANS in the presence of PrP27–30, dissociated and unfolded by increasing Gdn·HCl concentrations (Figures 1 and 2), indicates a decreasing fluorescence intensity with increasing concentrations of Gdn·HCl and a parallel large change in the wavelength of the ANS emission maximum from 493 to 534 nm (Figure 1 and inset of Figure 2). The intensity values at low Gdn·HCl concentrations are uncertain due to the turbidity and light scattering at <1 M Gdn·HCl. The intensity and emission wavelength maxima underwent a three-stage transition: a rapid decrease in intensity and an unchanged wavelength emission maximum between 0 and 2 M Gdn·HCl; a less steep decrease in intensity and a rapid red shift of the emission wavelength maximum between 2 and 4 M Gdn·HCl; and a final steady state with no further changes in intensity or the ANS emission maximum between 4 and 7 M Gdn·HCl.

There is a parallel between the fractional change (F_{app}) in turbidity and the ANS fluorescence intensity of PrP27–30 at low concentrations of Gdn·HCl (Figure 3). The PrP27–30 dissociated at 2 M Gdn·HCl had hydrophobic binding sites for ANS with little or no shift in the ANS emission wavelength, and the fluorescence intensity was 1.5–2× higher than that of the fully unfolded protein.

The data presented here, together with previous results of SE-HPLC (Safar et al., 1993a) obtained at the same protein concentration, indicate that PrP27–30 dissociates at low Gdn·HCl concentrations, and both the aggregated and dissociated forms of intermediate I_1 (Safar et al., 1993a) had hydrophobic binding sites for ANS. The dilution of PrP27–30 from 2 M Gdn·HCl solution or dialysis induced rapid association and aggregation (data not shown). The infectivity

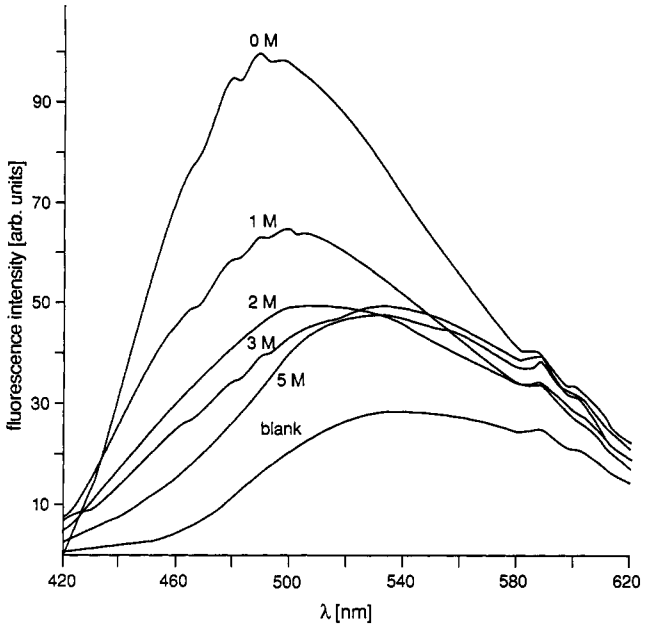

FIGURE 1: Fluorescence spectra of ANS during equilibrium dissociation and unfolding of PrP27–30 in Gdn·HCl. The aliquots of PrP27–30 with a final protein concentration of 4.3 μM were equilibrated for 24 h in the indicated concentrations of Gdn·HCl in TBS (pH 7.4) at 23 °C, and before recording, they were mixed with a concentrated stock of ANS dissolved in identical buffer. The excitation wavelength was 380 nm, and the final ANS concentration was 125 μM; the blank was a 125 μM solution of ANS in TBS (pH 7.4).

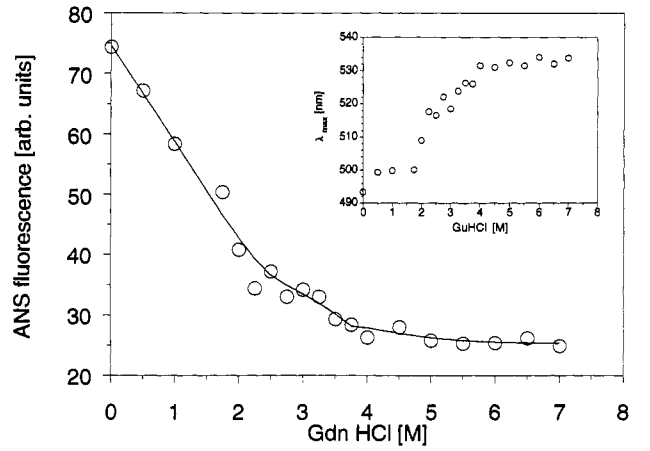

FIGURE 2: Changes in the ANS fluorescence intensity and emission maximum wavelength (inset) during equilibrium dissociation and unfolding of PrP27–30 plotted as a function of Gdn·HCl concentration. Aliquots of PrP27–30, of final protein concentration 4.3 μM, were equilibrated for 24 h with the indicated concentrations of Gdn·HCl in TBS (pH 7.4) at 23 °C, and before recording, they were mixed with final a 125 μM concentration of ANS, dissolved in the buffer with the corresponding concentration of Gdn·HCl. The excitation wavelength was 380 nm, and the emission wavelength was 490 nm.

of PrP27–30 first equilibrated in 2 M Gdn·HCl and then diluted 1000× was 8.1 ± 0.3 log ID_{50}/mL and did not significantly differ from that of the untreated original sample.

ANS Titration of Gdn·HCl-Induced Intermediate I_1. The ANS titration of the PrP27–30 I_1 intermediate at equilibrium in 2 M Gdn·HCl is shown in Figure 4. The fit of the data points between a 10^{-6} and 10^{-4} M concentration of ANS by Cogan's formula (data not shown) gave an apparent $K_D = 6.1 \times 10^{-6}$ M and 25 ANS molecules bound per molecule of PrP27–30. The titration results indicate multiple high-affinity hydrophobic binding sites of the equilibrium association

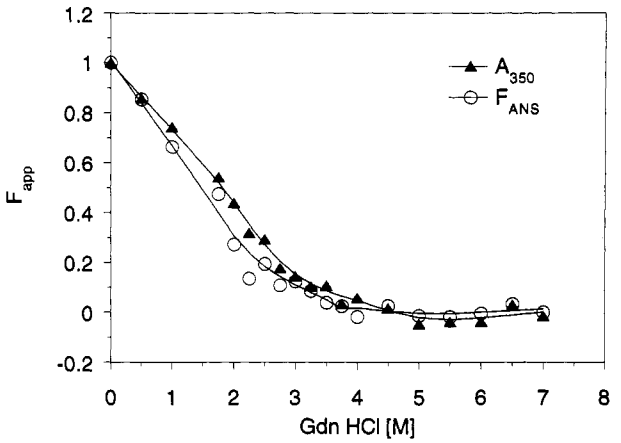

FIGURE 3: PrP27–30 equilibrium dissociation and unfolding in Gdn·HCl and, for comparison, expressed as a fractional change (F_{app}) in turbidity at 350 nm (▲) and ANS fluorescence intensity at 490 nm (○). PrP27–30 was equilibrated with increasing concentrations of Gdn·HCl in TBS (pH 7.4) for 24 h at 23 °C.

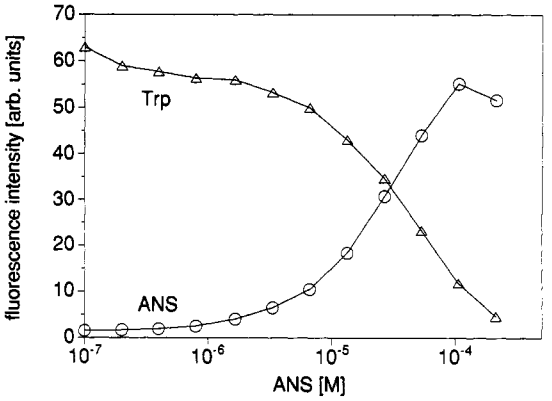

FIGURE 4: Titration of the dissociated equilibrium intermediate of PrP27–30 and quenching of the intrinsic fluorescence of Trp by ANS. Aliquots of PrP27–30 with a protein concentration of 4.3 μM were equilibrated for 24 h in 2 M Gdn·HCl in TBS (pH 7.4) at 23 °C and mixed with small aliquots of a concentrated stock of ANS in an identical buffer. The excitation wavelengths were 380 nm for ANS and 292 nm for Trp, and emission wavelengths were 490 nm for ANS and 340 nm for Trp.

intermediate I_1 of PrP27–30 for ANS. The relative decrease in fluorescence intensity at an ANS concentration $>10^{-4}$ M and the absorbance of ~1.3 probably indicate an inner filter effect due to the high dye concentration.

Quenching of Intrinsic Tryptophan Fluorescence of Gdn·HCl-Induced Intermediate I_1 by ANS. In 2 M Gdn·HCl, the intensity of the intrinsic fluorescence of Trp diminished in parallel with the increasing concentration of ANS after excitation at 292 nm (Figures 4 and 5). The quenching of the intrinsic fluorescence of the tryptophan of PrP27–30 association intermediate I_1 at low concentrations of ANS (Figure 4) and the nonlinear Stern–Volmer plot (data not shown) with a large static quenching component ($K_{sv} = 1.3 \times 10^4$ M^{-1}) both demonstrate that the quenching is due to the ANS binding and that some sites are in close proximity to the hydrophobic domain containing either one or both Trp residues.

HCl-Induced Dissociation of PrP27–30. Increasing the concentration of HCl in the presence of 100 mM NaCl dissociated PrP27–30 aggregates at pH <2.0, as judged from the decreased turbidity; the dissociated protein maintained a significant portion of its secondary structure (Figure 6). The amide band of the CD spectra of PrP27–30 recorded at pH 0.8–2.0 (Figure 7) was stable at 23 °C within 60 min of

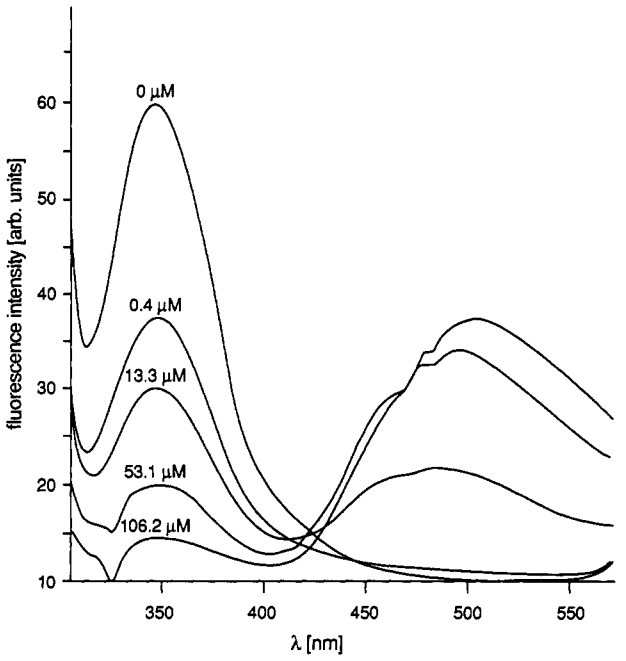

FIGURE 5: Representative fluorescence spectra of Trp in the Gdn·HCl-induced equilibrium intermediate of PrP27–30 and quenching by ANS. The aliquots of PrP27–30 with a protein concentration of 4.3 μM were equilibrated for 24 h in 2 M Gdn·HCl in TBS (pH 7.4) at 23 °C and mixed with small aliquots of a concentrated stock of ANS in an identical buffer. The excitation wavelength was 292 nm.

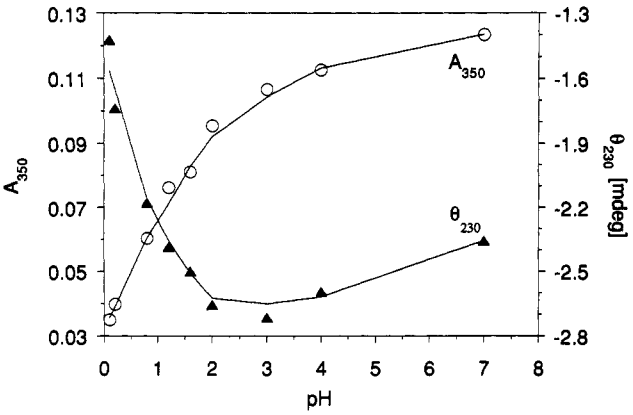

FIGURE 6: Dissociation of PrP27–30 at low pH induced by HCl and monitored by turbidity at 320 nm and CD spectroscopy at 230 nm. The small aliquots of PrP27–30 were diluted manually in 100 mM NaCl buffer and adjusted to the indicated pH with HCl. The protein concentration was 4.3 μM.

recording and demonstrated double minima at 222 and 208 nm, a crossover point at 201 nm, and a near-UV aromatic spectrum very close to the baseline. Decreasing the pH progressively diminished the [θ] and blue-shifted both negative minima and crossover points. Increasing the pH of the acid-induced PrP intermediate from 0.8 to 7.4 caused protein association, as indicated by an increase in the turbidity of the solution (data not shown) and visible sediment after overnight storage.

CD spectroscopy shows the presence of an acid-induced equilibrium intermediate of PrP27–30 (A-form) with a nonrandom secondary structure. There are no discernible aromatic bands in the spectra (Figure 7), reflecting insignificant tertiary structure interactions. The preliminary data recorded at pH 0.8 indicate the linear dependency of the ellipticity at 222 nm on the PrP27–30 concentration from 4.3 $\times 10^{-6}$ to 5.9 $\times 10^{-8}$ M (data not shown). This finding, together

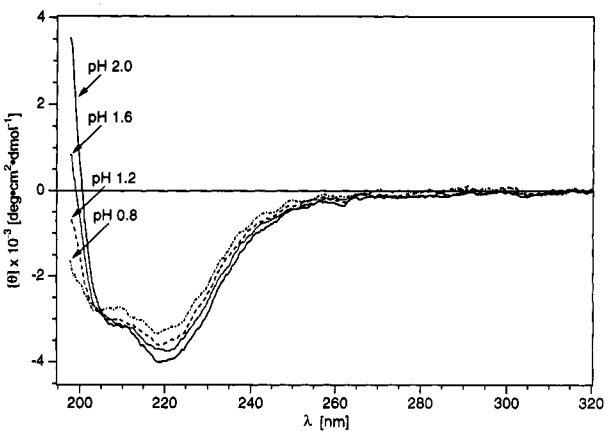

FIGURE 7: UV CD spectra of the acid-induced PrP27–30 intermediate at pH 0.8–2.0. The protein content used to calculate [θ] was monitored by the absorbance at 205 nm (Scopes, 1974) and corrected for turbidity. The small aliquots of PrP27–30 with a final protein concentration of 4.3 μM were diluted manually into 100 mM NaCl buffer and adjusted to the indicated pH with HCl.

with a stable $[\theta]_{208}/[\theta]_{222}$ ratio at different protein concentrations, suggests that PrP27–30 dissociates at low pH into monomers.

Temperature-Induced Unfolding of Gdn·HCl-Induced Intermediate I_1. PrP27–30 dissociated by 2 M Gdn·HCl in TBS (pH 7.4) was followed by turbidity measurements at 320 nm and CD spectroscopy at temperatures from 20 to 90 °C. The typical amide and aromatic CD spectra, shown in Figure 8 and recorded from 210 to 320 nm, demonstrated with increasing temperature a gradual loss of the negative amide band at 223–227 nm, a similar loss of the residual aromatic near-UV spectral pattern, and the gradual appearance of a negative trough toward ~210 nm (Figure 8). The absence of an isodichroic point suggests that the CD spectrum at 25 °C may represent the equilibrium of more than two conformations. In the single-wavelength experiments with the [θ] recorded at 222, 230, and 290 nm (upper two panels in Figure 9), the intermediate showed noncooperative and noncoincident transitions for all three parameters (left lower panel of Figure 9). Only [θ] recorded at 290 nm reached a plateau in the accessible temperature range.

Parallel experiments were performed on the previously studied α-lactalbumin (Ikeguchi et al., 1986; Pfeil, 1981). The native form of α-lactalbumin (right lower panel of Figure 9), scanned under identical conditions in TBS (pH 7.4), showed the typical cooperative transition with a melting point at ~63 °C. In contrast, the A-form of α-lactalbumin, prepared by lowering the pH to 2.0 with HCl, lost cooperativity in temperature unfolding studies. None of the samples of PrP27–30, when cooled back to 23 °C in the presence of 2 M Gdn·HCl, achieved refolding as judged by a persistent, large trough toward ~205 nm (Figure 10). The CD and absorbance spectroscopy of such samples kept at 23 °C for >16 h indicated irreversible precipitation. The samples cooled back to 23 °C and immediately diluted to 0.2 M Gdn·HCl also precipitated. The CD spectrum and turbidity obtained within 10 min after dilution indicated the formation of nonnative secondary and tertiary structure (Figure 10) and was rapidly followed by precipitation. The aliquot of heated and diluted PrP27–30 sample was tested in a bioassay in hamsters; at the time this paper was written, no animal had developed disease, indicating that the infectivity level is less than 2.9 log ID_{50}/mL, compared with 8.1 ± 0.3 log ID_{50}/mL for nonheated PrP27–30 equilibrated in 2 M Gdn·HCl.

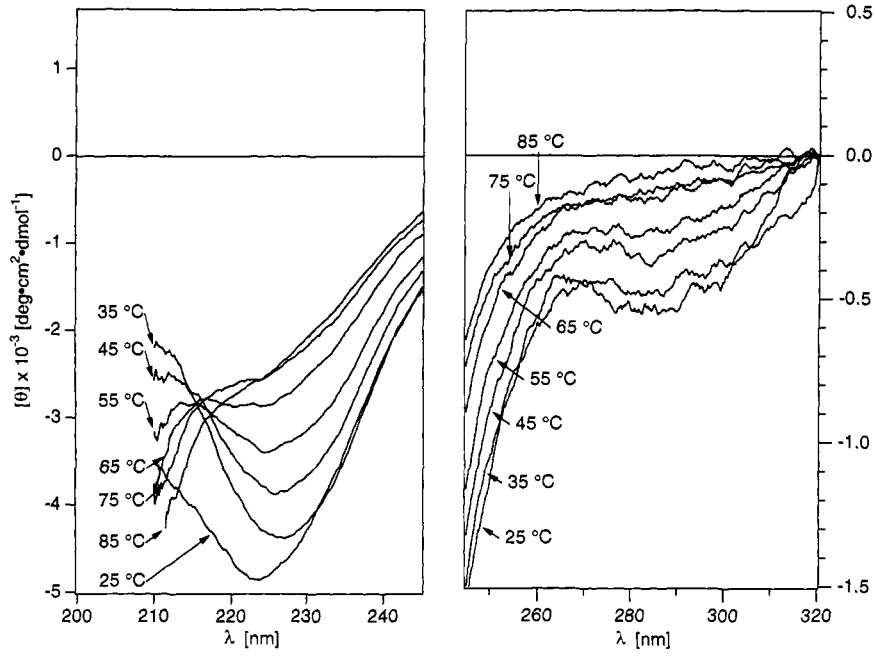

FIGURE 8: Amide (left panel) and aromatic (right panel) UV CD spectra of the Gdn·HCl-induced PrP27–30 equilibrium intermediate at different temperatures. The aliquots of PrP27–30 were equilibrated for 24 h in 2 M Gdn·HCl in TBS (pH 7.4) at 23 °C, degassed, and heated in a water-jacketed, 1-mm quartz cell. The protein concentration was 4.3 μM.

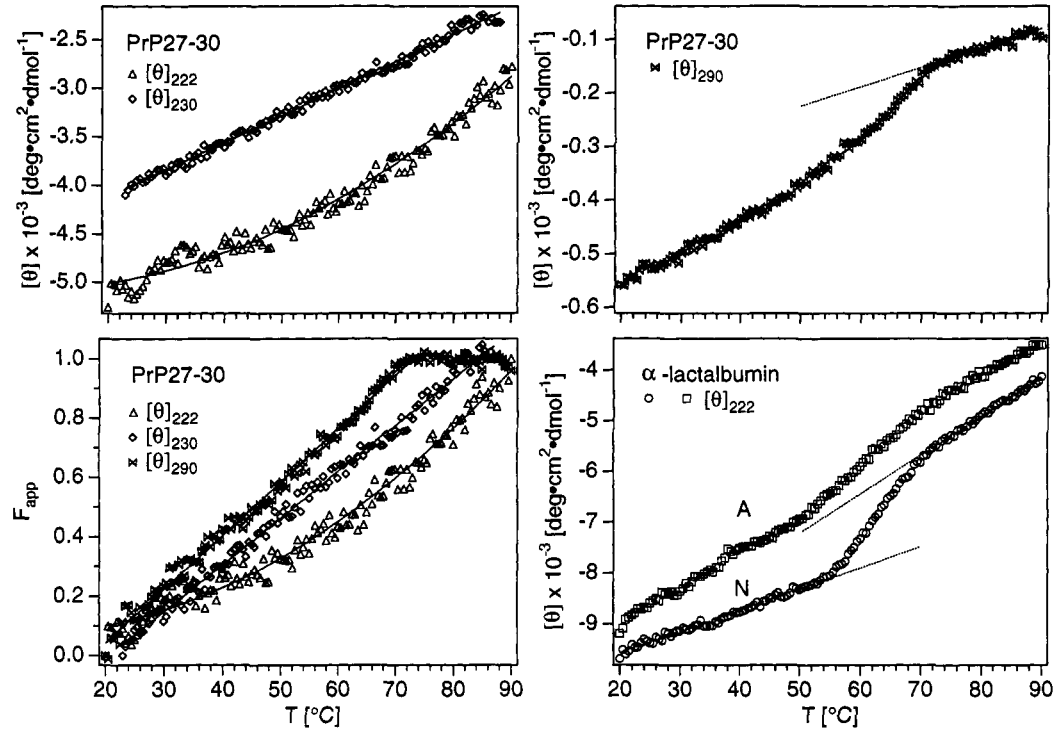

FIGURE 9: Temperature-induced unfolding of the Gdn·HCl-induced intermediate of PrP27–30 and α-lactalbumin. The unfolding of PrP27–30 was monitored by CD spectroscopy at 222, 230, and 290 nm (upper panels) and expressed as the apparent fractional change of unfolding, F_{app} (lower left panel). The temperature-induced unfolding of the native (N-form) and acid-induced conformational intermediate (A-form) forms of α-lactalbumin (Ikeguchi et al., 1986; Pfeil, 1981) was followed by CD spectroscopy at 222 nm (lower right panel). The aliquots of PrP27–30 were equilibrated with 2 M Gdn·HCl in TBS (pH 7.4) for 24 h at 23 °C, degassed, and heated in a water-jacketed, 1-mm quartz cell. The protein concentration was 4.3 μM; the curves are least-squares fits of the data.

The temperature-induced changes in the secondary and tertiary structure of the Gdn·HCl-induced equilibrium intermediate of PrP27–30 demonstrated very high thermodynamic stability and noncooperative unfolding, first of the residual elements of tertiary structure followed by the secondary structure elements. We cannot exclude the possibility that some residual secondary structure elements are present at temperatures above 90 °C (Figures 8 and 9).

Comparison of Secondary and Tertiary Structure of Gdn·HCl-Induced and HCl-Induced Equilibrium Intermediates and the PrP27–30 Aggregate. The amide CD spectra of PrP27–30 in 2 M Gdn·HCl were very similar to those of the acidic form, as characterized by negative minima and band intensities (Figure 10). Both CD spectra had significant negative ellipticity at 208 nm, indicating that a portion of the secondary structure exists in an α-helix and/or in β-turns. In

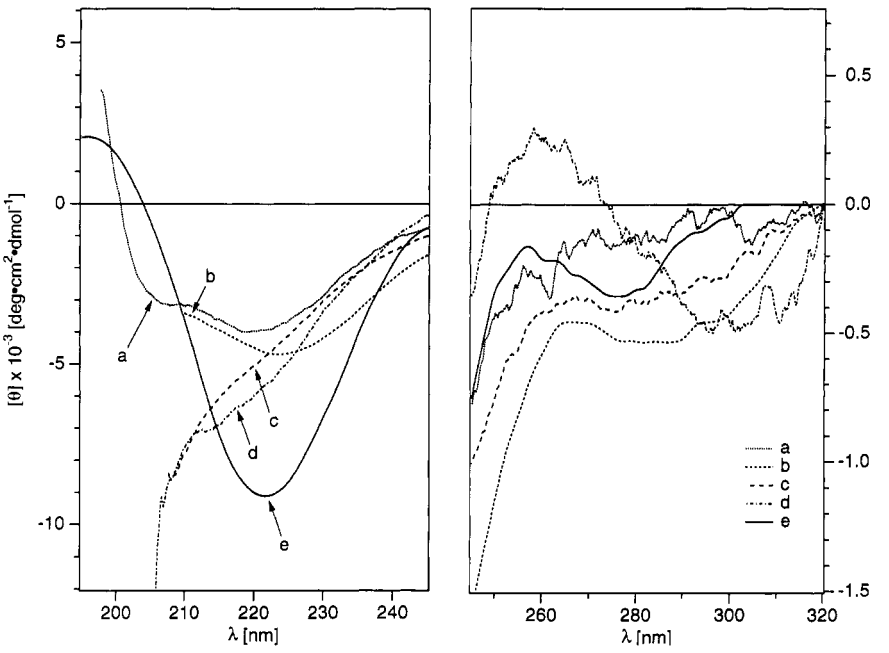

FIGURE 10: Representative amide (left panel) and aromatic (right panel) UV CD spectra of dissociated intermediate forms of PrP27–30 (a and b), thermally unfolded and reconstituted PrP27–30 intermediate forms (c and d), and PrP27–30 associated in a thin film (e). Shown are (a) the PrP27–30 in ~10 mM HCl and 100 mM NaCl (pH 2.0) at 23 °C; (b) the PrP27–30 in 2 M Gdn·HCl in TBS (pH 7.4) at 23 °C; (c) the PrP27–30 in 2 M Gdn·HCl in TBS (pH 7.4) heated to 90 °C, cooled to 23 °C, and recorded; (d) the PrP27–30 in 2 M Gdn·HCl in TBS (pH 7.4) heated to 90 °C, cooled to 23 °C, diluted 10× to 0.2 M Gdn·HCl, and recorded; and (e) the PrP27–30 film cast from 100 μL of a 9 μM solution in H_2O at 23 °C and dried in a vacuum in a desiccator above KOH pellets for 24 h. The PrP27–30 concentration in solution was 4.3 μM.

contrast, the amide CD spectra of PrP27–30 aggregated in a thin film had a single symmetrical negative minimum at 223 nm and insignificant ellipticity at 208 nm (Figure 10). This spectrum was previously (Safar et al., 1993a) assigned to the type II-β spectra (Stevens et al., 1968; Woody, 1985), and it has twice the ellipticity of the amide band of liposome-incorporated PrP27–30 (Safar et al., 1993a). The near-UV portion of the CD spectra of PrP27–30 associated in a thin film had a shallow negative band at 278 nm. The aromatic spectrum of the Gdn·HCl-induced equilibrium intermediate is similar; the negative aromatic band became broader and red-shifted to 292 nm. The aromatic bands of the CD spectra of the acidic intermediate are close to the baseline; the negative aromatic band between 278 and 292 nm disappeared.

The CD spectrum of acid, as well as of Gdn·HCl-induced intermediates of PrP27–30, indicates the presence of a substantial portion of the secondary structure, dissimilar to the aggregated PrP27–30. The apparent α-helical and/or β-turn component of the secondary structure of intermediates transformed in the associated PrP27–30 into "pure" type II-β spectra (Stevens et al., 1968; Woody, 1985), with little or no changes in the residual tertiary structure.

DISCUSSION

The conformation and characteristics of the equilibrium intermediates of PrP27–30 are critical for the following reasons: (a) they are the direct thermodynamic and conformational precursors of the scrapie amyloid aggregate; and (b) comparison of the monomeric intermediates and the PrP27–30 aggregate provides essential information about the stability, the mechanism of association, and accompanying conformational transitions. All attempts to directly follow the PrP27–30 and PrP^{Sc} refolding *in vitro* up to now have been unsuccessful [Safar et al. (unpublished results) and Prusiner et al. (1993)] due to the formation of misfolded aggregates.

The equilibrium dissociation and unfolding of PrP27–30 in increasing concentrations of Gdn·HCl, monitored in this study by ANS fluorescence (Semitsonov et al., 1991), indicated that the aggregated PrP27–30 and the dissociated monomeric intermediate I_1 had higher affinities for ANS than the intermediate I_2 and the protein in the unfolded state. Despite some artifacts introduced at lower than 1 M Gdn·HCl by light scattering, the large changes in ANS fluorescence intensity within experimental error paralleled changes in turbidity. We believe that the changes in ANS fluorescence intensity indicate the presence of more exposed hydrophobic residues and/or higher β-sheet content in aggregates than in the dissociated monomer I_1. Such an interpretation is supported by comparable fluorescence data obtained with ANS in α-lactalbumin (Mulqueen & Kronman, 1982) and β-lactoglobulin (Laligant et al., 1991), with 2-toluidinylnaphthalene-6-sulfonate (TNS) in poly(L-lysine) (Lynn & Fasman, 1968; Witz & Van Duuren, 1973), and with thioflavine T in β/A4 Alzheimer's amyloid (Levine, 1993). The large increase in β-sheet secondary structure content and the hydration dependency of the aromatic spectrum of aggregated PrP27–30, which we previously observed by CD spectroscopy (Safar et al., 1993b), confirm this conclusion. Thus, the changes in the CD spectrum match the perturbation in ANS fluorescence, and both suggest coupling of amyloid association of PrP27–30 and formation of β-sheet structure with more exposed hydrophobic side chains, resulting in higher affinity for ANS.

The experiments with ANS fluorescence and equilibrium unfolding of model monomeric proteins show fluorescence maxima concurrent with the transition zone of the protein from the folded to the unfolded state (Semitsonov et al., 1991; Uversky et al., 1992). The maximum is evidence of the compact or molten globule intermediate in the transition zone (Kuwajima, 1989; Ptitsyn et al., 1990). In contrast, there is no such expected transition zone or peak of ANS fluorescence during equilibrium unfolding of PrP27–30 in our experiments.

Instead, the maximum fluorescence is shifted to the lowest Gdn·HCl concentrations, where PrP27–30 occurs as an aggregate and dissociated intermediate I_1. The fluorescence titration and tryptophan quenching of the dissociated intermediate form of PrP27–30 by ANS showed that it had multiple, high-affinity, hydrophobic ANS binding sites, some in close proximity to one or both Trp residues. The results of ANS binding corroborate CD and Trp fluorescence spectroscopic evidence (Safar et al., 1993b) for PrP27–30 association through an equilibrium intermediate in a hydrophobic, nonnative, and nondenatured (molten globule-like) conformation.

Similar molten globule-like intermediate conformations of various proteins are observed in equilibrium at low pH (A-forms) (Kuwajima, 1989; Ptitsyn, 1991; Ptitsyn et al., 1990); they are stabilized by neutral salts (Fink et al., 1993; Goto & Fink, 1990). The dissociation of PrP27–30 aggregates at pH ≤2 in the presence of NaCl produced the acid-induced PrP27–30 intermediate (A-form), with secondary structure similar to that of the intermediate observed in low concentrations of Gdn·HCl. However, the A-form lost all of its residual tertiary structure interactions. The secondary structure estimate of the Gdn·HCl form and the A-form of PrP27–30 by deconvolution was not possible because of the high wavelength cutoffs. The prominent negative amide band at 208 nm suggests the presence of significant portions of the α-helical (Woody, 1985), type I(III) β-turn (Woody, 1985), or 3_{10}-helix-like (Miick et al., 1992) secondary structure elements in both intermediates. In contrast, this band is completely absent from associated or liposome-incorporated PrP27–30; the liposome-incorporated or aggregated solid state PrP27–30 is an all-β protein with ≥43% of the secondary structure present as β-sheets and the rest as β-turns or random coil conformations (Safar et al., 1993a). Comparison of the amide bands of CD spectra of intermediates and aggregated PrP27–30 provides evidence for a conformational transition during association, with transformation of some elements of the secondary structure into β-sheets. The existence of a stable intermediate form of PrP27–30 (A-form) at low pH is of interest because the cellular compartment in which normal-to-abnormal PrP conversion may occur *in vivo* is the endosome or lysosome (Borchelt et al., 1992; Caughey et al., 1991), with both compartments displaying physiologically low pH values. The mechanism of the acid-induced, native-to-molten globule transition has, in fact, been demonstrated for several proteins *in vitro* (Fink et al., 1993; Goto et al., 1990; Goto & Fink, 1990).

The important thermodynamic property of compact early kinetic intermediates of protein folding and their equilibrium forms (Kuwajima, 1989; Matthews, 1993a; Ptitsyn, 1991) is that there is little or no cooperativity during thermal unfolding (Haynie & Freire, 1993; Kuwajima et al., 1985; Pfeil, 1981). The Gdn·HCl-induced intermediate of PrP27–30 responded to heat by a gradual loss of secondary and residual tertiary structure with no signs of cooperativity. The CD spectroscopy followup of the PrP27–30 structure at three different wavelengths demonstrated noncoincidental conformational transitions, reported for intermediate conformational forms (Kuwajima, 1989; Ptitsyn, 1991). The residues of the tertiary structure were the least stable. In contrast, the PrP27–30 intermediate maintained some elements of secondary structure above 90 °C. The difference in the behavior of native and molten globule protein forms is well documented with the native form and acid-induced A-form of α-lactalbumin [this paper, Kuwajima et al. (1985), and Pfeil (1981)].

The irreversibility of temperature unfolding of the PrP27–30 intermediate is striking and difficult to explain. Unfolded protein formed partially folded "wrong" aggregates at low temperature after high-temperature unfolding and/or after dilution from high to low Gdn·HCl concentration. Similar results were obtained after dialysis, in the presence or absence of detergents or phospholipids [Safar et al. (unpublished data) and Prusiner et al. (1993)]. The failure to refold the protein *in vitro* may indicate the absence of a required folding cofactor. However, a simple reason may be the covalently attached C-terminal glycolipid. We have observed glycolipid-mediated oligomerization of PrP27–30 at ≥3 M Gdn·HCl, and this phenomenon may increase the chance of short-distance hydrophobic interactions during the early stages of refolding and the formation of misfolded aggregates.

The molten globule state of a protein is structurally and thermodynamically distinct from both the native and denatured states; it is defined as a compact, partly ordered conformation with nonspecific tertiary structure, a high content of secondary structure, significant structural flexibility, and a tendency to aggregate due to the more exposed hydrophobic surface (Barrick & Baldwin, 1993; Kuwajima, 1989; Ptitsyn, 1991). The characteristics of the scrapie amyloid (prion) protein intermediate, dissociated from aggregates at low concentrations of Gdn·HCl or by decreasing pH, meet this definition. The conformations defined as molten globules exist either as early kinetic protein folding intermediates (Matthews, 1993b) or equilibrium intermediates (Barrick & Baldwin, 1993; Kuwajima, 1989; Ptitsyn, 1991). The compact early kinetic intermediates of protein folding pathways occur during the early folding phase (Matthews, 1993b) and are probably the universal step in protein folding. The conformationally similar metastable protein forms appear in equilibrium in some apoproteins (Baum et al., 1989; Ikeguchi et al., 1986) or are stabilized at equilibrium by low concentrations of Gdn·HCl (Kuwajima, 1989; Semitsonov et al., 1991; Uversky et al., 1992), by low pH (A-forms) (Fink et al., 1993; Goto et al., 1990; Goto & Fink, 1990), or by interaction with chaperonins (Martin et al., 1991; Park et al., 1993). Which mechanism is involved in the formation of the monomeric molten globule intermediate of scrapie amyloid (prion) protein and the resulting aggregation is the critical question of the pathogenesis of the disease.

CONCLUSIONS

The data presented in this and a previous paper (Safar et al., 1993a) have several implications for scrapie amyloid formation: (1) scrapie amyloid (prion) protein apparently is formed through a hydrophobic, nonnative, nondenatured conformational intermediate with molten globule-like CD characteristics; (2) this intermediate has an intrinsically unstable tertiary structure and a tendency to aggregate; (3) the secondary structure of this thermodynamic and conformational amyloid precursor contains a significant portion of non-β-sheet elements; (4) the association, probably triggered by hydrophobic interactions and the alignment of intermolecular β-sheets, induces reshuffling in the tertiary and secondary structure into an "all-β" conformation with more exposed hydrophobic side chains and higher affinity for ANS; (5) the stability of the secondary structure of the monomeric intermediate apparently is increased by association, and therefore the PrP27–30 aggregate may represent a thermodynamically trapped folding intermediate; and (6) the conformational intermediate of PrP27–30 with molten globule-

like CD characteristics is also induced by low pH (A-form) in the presence of salts.

ACKNOWLEDGMENT

The authors thank Drs. R. Chen and H. Arnheiter for critical review of the manuscript, Al Bacote and Elise Bowman for excellent technical assistance, Devera G. Schoenberg for editing the manuscript, and Steve Ono for document production assistance.

REFERENCES

Barrick, D., & Baldwin, R. L. (1993) *Protein Sci. 2,* 869–876.
Baum, J., Dobson, C. M., Evans, P. A., & Hanley, C. (1989) *Biochemistry 28,* 7–13.
Borchelt, D. R., Taraboulos, A., & Prusiner, S. B. (1992) *J. Biol. Chem. 267,* 16188–16199.
Caughey, B., Raymond, G. J., Ernst, D., & Race, R. E. (1991) *J. Virol. 65,* 6597–6603.
Cogan, U., Kopelman, M., Mokady, S., & Shinitzki, M. (1976) *Eur. J. Biochem. 65,* 71–78.
Creighton, T. E. (1990) *Biochem. J. 270,* 1–16.
Edwards, R. A., & Woody, R. W. (1979) *Biochemistry 18,* 5197–5204.
Eftink, M. R., & Ghiron, C. A. (1976) *J. Phys. Chem. 80,* 486–493.
Fink, A. L., Calciano, L., Goto, Y., Nishimura, M., & Swedberg, S. A. (1993) *Protein Sci. 2,* 1155–1160.
Gajdusek, D. C. (1988) *Mt. Sinai J. Med. 55,* 3–5.
Glenner, G. G., & Murphy, M. A. (1989) *J. Neurol. Sci. 94,* 1–28.
Goto, Y., & Fink, A. L. (1990) *J. Mol. Biol. 214,* 803–805.
Goto, Y., Calciano, L. J., & Fink, A. L. (1990) *Proc. Natl. Acad. Sci. U.S.A. 87,* 573–577.
Haynie, D. T., & Freire, E. (1993) *Proteins: Struct., Funct., Genet. 16,* 115–140.
Ikeguchi, M., Kuwajima, K., Mitani, M., & Sugai, S. (1986) *Biochemistry 25,* 6965–6972.
Jaenicke, R. (1987) *Prog. Biophys. Mol. Biol. 49,* 117–237.
Jaenicke, R. (1991) *Biochemistry 30,* 3147–3161.
Kuwajima, K. (1989) *Proteins: Struct., Funct., Genet. 6,* 87–103.
Kuwajima, K., Hiraoka, Y., Ikeguchi, M., & Sugai, S. (1985) *Biochemistry 24,* 874–881.
Laligant, A., Dumay, E., Valencia, C. C., Cuq, J.-L., & Cheftel, J.-C. (1991) *J. Agric. Food Chem. 39,* 2147–2155.
Lansbury, P. T., Jr. (1992) *Biochemistry 31,* 6865–6870.
Levine, H. (1993) *Protein Sci. 2,* 404–410.
Lynn, J., & Fasman, G. D. (1968) *Biochem. Biophys. Res. Commun. 33,* 327–334.
Mann, C. J., & Matthews, C. R. (1993) *Biochemistry 32,* 5282–5290.
Martin, J., Langer, T., Boteva, R., Schramel, A., Horwich, A. L., & Hartl, F.-U. (1991) *Nature 352,* 36–42.
Matthews, B. W. (1993a) *Annu. Rev. Biochem. 62,* 139–160.
Matthews, C. R. (1993b) *Annu. Rev. Biochem. 62,* 653–683.
Matthews, C. R., & Crisanti, M. M. (1981) *Biochemistry 20,* 784–792.
Miick, S. M., Martinez, G. V., Fiori, W. R., Todd, A. P., & Millhauser, G. L. (1992) *Nature 359,* 653–655.
Mulqueen, P. M., & Kronman, M. J. (1982) *Arch. Biochem. Biophys. 215,* 28–39.
Pace, C. N. (1986) *Methods Enzymol. 131,* 266–280.
Pan, K.-M., Baldwin, M., Nguyen, J., Gasset, M., Serban, A., Groth, D., Mehlhorn, I., Huang, Z., Fletterick, R. J., Cohen, F. E., & Prusiner, S. B. (1993) *Proc. Natl. Acad. Sci. U.S.A. 90,* 10962–10966.
Park, K., Flyn, G. C., Rothman, J. E., & Fasman, G. D. (1993) *Protein Sci. 2,* 325–330.
Pfeil, W. (1981) *Biophys. Chem. 13,* 181–186.
Prusiner, S. B. (1993) *Arch. Neurol. 50,* 1129–1153.
Prusiner, S. B., McKinley, M. P., Bowman, K. A., Bolton, D. C., Bendheim, P. E., Groth, D. F., & Glenner, G. G. (1983) *Cell 35,* 349–358.
Prusiner, S. B., Groth, D., Serban, A., Stahl, N., & Gabizon, R. (1993) *Proc. Natl. Acad. Sci. U.S.A. 90,* 2793–2797.
Ptitsyn, O. B. (1991) *FEBS Lett. 285,* 176–181.
Ptitsyn, O. B., Pain, R. H., Semitsonov, G. V., Zerovnik, E., & Razgulyaev, O. I. (1990) *FEBS Lett. 262,* 20–24.
Safar, J., Wang, W., Padgett, M. P., Ceroni, M., Piccardo, P., Zopf, D., Gajdusek, D. C., & Gibbs, C. J., Jr. (1990) *Proc. Natl. Acad. Sci. U.S.A. 87,* 6373–6377.
Safar, J., Ceroni, M., Gajdusek, D. C., & Gibbs, C. J., Jr. (1991) *J. Infect. Dis. 163,* 488–94.
Safar, J., Roller, P. P., Gajdusek, D. C., & Gibbs, C. J., Jr. (1993a) *J. Biol. Chem. 268,* 20276–20284.
Safar, J., Roller, P. P., Gajdusek, D. C., & Gibbs, C. J., Jr. (1993b) *Protein Sci. 2,* 2206–2216.
Safar, J., Roller, P. P., Ruben, G. C., Gajdusek, D. C., & Gibbs, C. J., Jr. (1993c) *Biopolymers 33,* 1461–1476.
Scopes, R. K. (1974) *Anal. Biochem. 59,* 277–282.
Semitsonov, G. V., Rodionova, N. A., Razgulyaev, O. I., Uverski, V. N., Gripas, A. F., & Gilmanshin, R. I. (1991) *Biopolymers 31,* 119–128.
Stahl, N., Borchelt, D. R., & Prusiner, S. B. (1990) *Biochemistry 29,* 5405–12.
Stevens, E. S. (1977) *Methods Enzymol. 49,* 214–221.
Stevens, L., Townend, R., Timasheff, S. N., Fasman, G. D., & Potter, J. (1968) *Biochemistry 7,* 3717–3720.
Turk, E., Teplow, D. B., Hood, L. E., & Prusiner, S. B. (1988) *Eur. J. Biochem. 176,* 21–30.
Uversky, V. N., Semisotnov, G. V., Pain, R. H., & Ptitsyn, O. B. (1992) *FEBS Lett. 314,* 89–92.
Weissmann, C. (1991) *Nature 352,* 679–683.
Witz, G., & Van Duuren, B. L. (1973) *J. Phys. Chem. 77,* 648–651.
Woody, R. W. (1985) in *Conformation in Biology and Drug Design* (Udenfriend, S., & Meienhofer, J., Eds.) pp 15–114, Academic Press, New York.
Wu, F. Y.-H., & Wu, C.-W. (1978) *Biochemistry 17,* 138–144.